J. Fluid Mech. (1991), *vol.* 225, *pp.* 529–543
Printed in Great Britain

Distortion of line and surface elements in model turbulent flows

By I. T. DRUMMOND AND W. MÜNCH
Department of Applied Mathematics and Theoretical Physics, University of Cambridge, Silver Street, Cambridge CB3 9EW, UK

(Received 2 October 1989 and in revised form 7 September 1990)

Material lines and surfaces transported in a random velocity field undergo bending and stretching. In this paper we investigate the time evolution of curvature in line and surface elements both analytically and by numerical simulation for a simple model turbulence. Our analysis is close to that of Pope (1988) for the evolution of curvature in surface elements. We show that the equation governing the evolution of curvature in a line element is very similar to that governing the evolution of the principal curvature in a surface patch. We investigate the circumstances in which the effect of straining fluctuations is to cause the exponential rate of growth of curvature discovered by Pope *et al.* (1989). Our simulation confirms that the presence of helicity in the turbulent flow results in the development of a non-vanishing mean torsion in a line element. The results of the simulation also suggest that the generation of curvature tends to occur in regions different from those associated with rapid stretching. The generation of torsion, however, is found not to be correlated with either bending or stretching.

1. Introduction

In a previous paper (Drummond & Münch 1990) we analysed the stretching of line and surface elements in turbulent flows. We were able to demonstrate that the mean length or surface area and its higher statistical moments grow exponentially after some initial period of time and that higher statistical moments of the length or surface area grow faster than lower moments. Furthermore we constructed a numerical model illustrating the importance of the time-reversal invariance of the turbulent flow and its breakdown, for the relationship of between the stretching of line and surface elements. In this paper we examine both analytically and by numerical experiment the development of curvature in line and surface elements and how the evolution of curvature and torsion is related to the stretching of a line or surface element transported in a turbulent velocity field. We also examine the appearance of torsion and the manner in which it responds to the presence of helicity in the turbulent flow. In the numerical simulations we use a kinematical turbulence model which is generated as a sum of Fourier components based on the ideas of Kraichnan (1970) and Drummond, Duane & Horgan (1984). Although this is not a particularly realistic model of a turbulent velocity field it is very useful for illustrating some of the important features of the problems related to the development of curvature and torsion in turbulent flows.

In §2 we set out the differential equations governing the time development of various quantities of interest, and in §3 we derive equations for the time development of the curvature of line and surface elements. We indicate the structure of our velocity field in §4 and the numerical results on the development of curvature for

both line and surface elements are presented in §5. In §6 we briefly discuss the evolution of torsion of a line element in both helical and non-helical flows. In §7 we show some of the correlation functions between the curvature, stretching and the torsion. Section 8 concludes.

2. Time development of line and surface elements

In a recent paper Pope (1988) has set out an approach to computing the properties of surface elements. Our investigation is essentially along the same lines but deals also with line elements. For completeness and clarity we set out our version of the relevant equations below.

A curve in space at time t may be written in the parametric form

$$\boldsymbol{r} = \boldsymbol{r}(\lambda, t). \tag{1}$$

At time $t = 0$, we may give the parameter λ the interpretation of the distance along the curve. The line element vector is $\boldsymbol{l}$ where

$$\boldsymbol{l} = \frac{\partial \boldsymbol{r}}{\partial \lambda}. \tag{2}$$

A point carried by the fluid flow satisfies

$$\frac{\mathrm{d}}{\mathrm{d}t}\boldsymbol{r} = \boldsymbol{u}(\boldsymbol{r}, t), \tag{3}$$

where $\boldsymbol{u}(\boldsymbol{r}, t)$ is the velocity field.

The equation for the line element $\boldsymbol{l}$ is

$$\dot{l}_i = W_{ij} l_j, \tag{4}$$

where

$$W_{ij} = \frac{\partial}{\partial x_j} u_i. \tag{5}$$

It has the formal solution

$$l_i(t) = U_{ij}(t)\, l_j(0) \tag{6}$$

where the matrix $\boldsymbol{U}(t)$ satisfies the differential equation

$$\dot{\boldsymbol{U}}(t) = \boldsymbol{W}(t)\, \boldsymbol{U}(t) \tag{7}$$

and the boundary condition $\boldsymbol{U}(0) = 1$.

We shall also be interested in the higher-order quantities

$$\boldsymbol{a} = \frac{\partial}{\partial \lambda}\boldsymbol{l} = \frac{\partial^2}{\partial \lambda^2}\boldsymbol{r}, \tag{8}$$

and

$$\boldsymbol{b} = \frac{\partial}{\partial \lambda}\boldsymbol{a} = \frac{\partial^3}{\partial \lambda^3}\boldsymbol{r}, \tag{9}$$

which are needed in order to compute curvature and torsion. They obey the equations

$$\dot{a}_i = W_{ij} a_j + W_{ijk} l_j l_k \tag{10}$$

and

$$\dot{b}_i = W_{ij} b_j + 3 W_{ijk} l_j a_k + W_{ijkm} l_j l_k l_m, \tag{11}$$

where

$$W_{ijk} = \frac{\partial^2}{\partial x_j \partial x_k} u_i \tag{12}$$

and

$$W_{ijkm} = \frac{\partial^3}{\partial x_j \partial x_k \partial x_m} u_i. \tag{13}$$

If we denote the length of $\boldsymbol{l}$ by ξ then

$$\xi = \frac{\partial}{\partial \lambda} s, \tag{14}$$

where s is the distance measured along the curve at time t. We have

$$\frac{\partial}{\partial s} = \xi^{-1} \frac{\partial}{\partial \lambda}. \tag{15}$$

The unit tangent vector is

$$\boldsymbol{t} = \frac{\partial}{\partial s} \boldsymbol{r} = \xi^{-1} \boldsymbol{l}. \tag{16}$$

We also introduce a unit normal $\boldsymbol{n}$ and a bi-normal $\boldsymbol{m} = \boldsymbol{t} \wedge \boldsymbol{n}$. The three orthogonal unit vectors satisfy the Frenet formulae

$$\frac{\partial}{\partial s} \begin{pmatrix} \boldsymbol{t} \\ \boldsymbol{n} \\ \boldsymbol{m} \end{pmatrix} = \begin{pmatrix} 0 & \kappa & 0 \\ -\kappa & 0 & \tau \\ 0 & -\tau & 0 \end{pmatrix} \begin{pmatrix} \boldsymbol{t} \\ \boldsymbol{n} \\ \boldsymbol{m} \end{pmatrix}, \tag{17}$$

where κ is the curvature and τ the torsion.

It is easy to check that

$$\kappa n_i = \xi^{-2}(a_i - \xi^{-2} l_i l_j a_j), \tag{18}$$

so that, in magnitude,

$$\kappa = \xi^{-3} |\boldsymbol{l} \wedge \boldsymbol{a}|. \tag{19}$$

We have also

$$\tau = \boldsymbol{t} \wedge \boldsymbol{n} \cdot \frac{\partial}{\partial s} \boldsymbol{n}, \tag{20}$$

which yields the result

$$\tau = \frac{\boldsymbol{l} \wedge \boldsymbol{a} \cdot \boldsymbol{b}}{(\boldsymbol{l} \wedge \boldsymbol{a})^2}. \tag{21}$$

To investigate the properties of line elements our procedure is to generate an example of the turbulent velocity field, choose appropriate initial data for $\boldsymbol{r}$, $\boldsymbol{l}$, $\boldsymbol{a}$, and $\boldsymbol{b}$ and integrate numerically the above differential equations computing ξ, κ and τ at each stage.

Surfaces can be treated similarly. They require two parameters,

$$\boldsymbol{r} = \boldsymbol{r}(\lambda_1, \lambda_2, t). \tag{22}$$

This leads to two line elements

$$\boldsymbol{l}_a = \frac{\partial}{\partial \lambda_a} \boldsymbol{r}, \tag{23}$$

where $a = 1, 2$. Each $\boldsymbol{l}_a$ evolves according to (4) but from different initial data. The unit normal to the surface is $\boldsymbol{N}$ where

$$\boldsymbol{l}_1 \wedge \boldsymbol{l}_2 = A \boldsymbol{N}, \tag{24}$$

and A is the area of the surface element spanned by $\boldsymbol{l}_1$ and $\boldsymbol{l}_2$.

The quantities of interest are the principal extrinsic curvatures of the surface, k_1 and k_2, and the Gaussian or intrinsic curvature $K = k_1 k_2$. To extract these quantities we are required to achieve the simultaneous diagonalization of two quadratic forms, namely, the metric

$$g_{ab} = \boldsymbol{l}_a \cdot \boldsymbol{l}_b \tag{25}$$

and
$$h_{ab} = -\frac{\partial \boldsymbol{N}}{\partial \lambda_a} \cdot \boldsymbol{l}_b. \tag{26}$$

That is the principal curvatures k satisfy the eigenvalue equation

$$(\boldsymbol{h} - k\boldsymbol{g})\, x = 0, \tag{27}$$

where x is a two-dimensional eigenvector.

In terms of the quadratic forms the Gaussian curvature is defined by

$$K = \frac{\det \boldsymbol{h}}{\det \boldsymbol{g}} \tag{28}$$

and the principal curvatures are the solutions of the quadratic equation

$$k^2 - 2Hk + K = 0 \tag{29}$$

where
$$H = \tfrac{1}{2} \operatorname{tr} (\boldsymbol{g}^{-1}\boldsymbol{h}), \tag{30}$$

namely,
$$k_1 = H + (H^2 - K)^{\frac{1}{2}}, \quad k_2 = H - (H^2 - K)^{\frac{1}{2}}. \tag{31}$$

Again our procedure is to integrate the equations for $\boldsymbol{l}_1$ and $\boldsymbol{l}_2$ and compute the curvatures for each t in appropriately chosen velocity fields.

3. Time development of curvature

Pope (1988) has discussed an equation governing the time development of extrinsic curvature in surfaces. In fact, a similar equation holds for the time development of curvature in line elements also. It is convenient to present here a derivation of both cases.

From (18) we deduce that

$$\dot{\kappa} n_i + \kappa \dot{n}_i = -2\gamma\kappa n_i + \xi^{-2}(\dot{a}_i - \xi^{-2}\dot{l}_i l_j a_j) + \xi^{-4} l_i (2\gamma l_j a_j - \dot{l}_j a_j - l_j \dot{a}_j), \tag{32}$$

where
$$\gamma = \frac{\dot{\xi}}{\xi}. \tag{33}$$

Taking the scalar product with $\boldsymbol{n}$ we find

$$\dot{\kappa} = -2\gamma\kappa + \xi^2 n_i (\dot{a}_i - \xi^{-2}\dot{l}_i l_j a_j). \tag{34}$$

From (4) and (8) we find

$$\dot{\kappa} = -(2\gamma - W_{ij} n_i n_j)\,\kappa + W_{ijk} n_i t_j t_k. \tag{35}$$

Since
$$\gamma = W_{ij} t_i t_j, \tag{36}$$

we see that (34) involves only components of W_{ij} and W_{ijk} evaluated in the local frame of the line element. It becomes

$$\dot{\kappa} = -(2W_{ij} t_i t_j - W_{ij} n_i n_j)\,\kappa + W_{ijk} n_i t_j t_k. \tag{37}$$

The corresponding equation for surfaces is obtained by first differentiating (27) with respect to time. We normalize so that

$$x^{\mathrm{T}} \boldsymbol{g} x = 1. \tag{38}$$

We have then
$$\dot{k}\boldsymbol{g}x = (\dot{\boldsymbol{h}} - k\dot{\boldsymbol{g}})\, x + (\boldsymbol{h} - k\boldsymbol{g})\, \dot{x}. \tag{39}$$

Using the eigenvalue condition we find

$$\dot{k} = x^{\mathrm{T}} (\dot{\boldsymbol{h}} - k\dot{\boldsymbol{g}})\, x. \tag{40}$$

Now
$$\dot{g}_{ab} = 2S_{ij}\, l_{ai}\, l_{bj}, \tag{41}$$

where
$$S_{ij} = \tfrac{1}{2}(W_{ij} + W_{ji}). \tag{42}$$

We also have
$$\dot{h}_{ab} = W_{ijk} N_i\, l_{aj}\, l_{bk} - \hat{\gamma} h_{ab}, \tag{43}$$

where
$$\hat{\gamma} = \frac{\dot{A}}{A} = -W_{ij} N_i N_j. \tag{44}$$

Setting $\boldsymbol{x} = (x_1, x_2)$ and defining the unit vector corresponding to the principal curvature κ to be

$$\boldsymbol{e} = x_a \boldsymbol{l}_a \tag{45}$$

we see that
$$\dot{k} = -(2W_{ij}\, e_i\, e_j + \hat{\gamma})\, k + W_{ijk} N_i\, e_j\, e_k. \tag{46}$$

This in our notation is the equation derived by Pope (1988). It can be put in the form

$$\dot{k} = -(2W_{ij}\, e_i\, e_j - W_{ij} N_i N_j)\, k + W_{ijk} N_i\, e_j\, e_k. \tag{47}$$

Note the close similarity of form between (37) and (46). The two results are not identical, however, since the evolution in time of the two vectors $\boldsymbol{e}$ and $\boldsymbol{N}$ is different from that of the vectors $\boldsymbol{t}$ and $\boldsymbol{n}$. Nevertheless we might expect that, in isotropic turbulence where averaging over the orientation of local reference frame is plausible, the extrinsic principal curvature of a surface element and the curvature of a line element will develop in similar ways on the average. This is particularly clear in the short-time behaviour where the isotropy guarantees similar time development for the moments of either kind of curvature.

We have for small times t from (19)

$$\kappa^2 \approx (\epsilon_{ijk}\, W_{jlm}(0)\, t_l\, t_m\, t_k)^2\, t^2. \tag{48}$$

If we exploit the isotropy of the turbulence we find

$$\langle \kappa^2 \rangle \approx \tfrac{6}{35} \langle (W_{ijk})^2 \rangle\, t^2. \tag{49}$$

A similar argument for the principal curvatures of the area element yields

$$\langle k_1^2 + k_2^2 \rangle = 2k^2 \approx \tfrac{8}{35} \langle (W_{ijk})^2 \rangle\, t^2. \tag{50}$$

It follows that in both cases the root-mean-square curvature increases linearly with time. This will continue to be the case until a point in time is reached comparable with the correlation time of the turbulent velocity field. Beyond this point the form of the evolution will depend on the details of the turbulent velocity ensemble.

We can gain some insight into the curvature evolution by following arguments of a type suggested by Pope (1988). For example the second term in either (37) or (46) depends on the second derivative along the curve or surface of the normal component of the velocity field. It is naturally to be thought of as a bending term. This term fluctuates in a random way but is subject to time-independent statistics with a correlation time related to that of the velocity field. Were this the only term to affect the curvature the result would be a random walk for either κ or k. In such circumstances we would find

$$\langle \kappa^2 \rangle \approx \langle k^2 \rangle \propto t. \tag{51}$$

The first term in either (37) or (46) represents the effect straining on curvature. In a previous paper (Drummond & Münch 1990) we found that line or surface elements preferentially align themselves in the direction of maximum strain. Because of this the average value of the coefficient in the curvature term is negative. Were the influence of this coefficient on the statistical time development of the curvature to be

dominated by its average value the net effect would be a suppression of curvature. We would then expect the competition between the straining term and the bending term to lead to a finite asymptotic value for the mean-square curvature. However as emphasized by Pope, Yeung & Girimaji (1989) it is in no way obvious that this suppression occurs in practice and indeed they found in simulations that the r.m.s. curvature increased apparently unboundedly with time. We can examine this question in more detail by analysing the Pope equation for curvature development.

Let us express the curvature equations in the generic form

$$\dot{y} = A(t)\, y + B(t), \tag{52}$$

where y stands for whichever curvature we are interested in, $A(t)$ represents the straining term and $B(t)$ represents the bending term. For simplicity of exposition we will assume that $A(t)$ and $B(t)$ obey Gaussian statistics. The Gaussian restriction can easily be modified with no qualitative change in the conclusions provided we assume that the higher cumulant functions die away sufficiently rapidly with increasing order. This does have to be an assumption since otherwise it is possible to construct counter-examples to the results. However, since the velocity ensembles we use in this paper are Gaussian at the Eulerian level it is reasonable to assume that the corresponding Lagrangian quantities have the required properties. It is also plausible that the same is true for real turbulence. We have then

$$\begin{aligned} \langle A(t)\rangle &= -\Gamma, \\ \langle B\rangle &= 0, \\ \langle A(t)A(t')\rangle_{\mathrm{C}} &= F(t-t'), \\ \langle A(t)B(t')\rangle_{\mathrm{C}} &= G(t-t'), \end{aligned} \tag{53}$$

where $\langle A(t)A(t')\rangle_{\mathrm{C}}$ stands for the cumulant of $A(t)$,

$$\langle A(t)A(t')\rangle_{\mathrm{C}} = \langle A(t)A(t')\rangle - \langle A(t)\rangle\langle A(t')\rangle, \tag{54}$$

and similarly for the AB correlator. We assume of course that $\Gamma > 0$.

The solution of the homogeneous equation ($B(t) \equiv 0$) that obeys the boundary condition $y(t') = 1$ is

$$y(t,t') = \mathrm{e}^{\phi(t,t')}, \tag{55}$$

where

$$\phi(t,t') = \int_{t'}^{t} \mathrm{d}t''\, A(t''). \tag{56}$$

The solution of the complete equation that satisfies $y(0) = 0$ is

$$y(t) = \int_0^t \mathrm{d}t'\, \mathrm{e}^{\phi(t,t')} B(t'). \tag{57}$$

When $y(t)$ is sufficiently large we can neglect the bending term relative to the straining term. The behaviour of $y(t)$ is then effectively determined by the homogeneous equation. The results for the solution of the complete equation can readily be inferred from this analysis,

$$y(t) \propto \mathrm{e}^{\phi(t)}, \tag{58}$$

where

$$\phi(t) \equiv \phi(t,0) = \int_0^t \mathrm{d}t'\, A(t'). \tag{59}$$

It follows that the pth moment of $y(t)$ is

$$\langle (y(t))^p\rangle \propto \langle \mathrm{e}^{p\phi(t)}\rangle = \exp\left[p\langle\phi(t)\rangle + \tfrac{1}{2}p^2\langle(\phi(t))^2\rangle_{\mathrm{C}}\right], \tag{60}$$

where we have made use of the assumed Gaussian nature of the statistics for $A(t)$. We have

$$\langle \phi(t) \rangle = -\Gamma t \tag{61}$$

and

$$\begin{aligned} \langle (\phi(t))^2 \rangle_{\mathrm{C}} &= \int_0^t \mathrm{d}t' \int_0^t \mathrm{d}t'' F(t'-t'') \\ &\sim t \int_{-\infty}^{\infty} \mathrm{d}t' F(t') \\ &= C_A t, \end{aligned} \tag{62}$$

the asymptotic form being appropriate for large t. If we introduce an integral timescale τ_A for A-correlations we can set

$$C_A = \langle (A(0))^2 \rangle_{\mathrm{C}} \tau_A. \tag{63}$$

It follows that in this limit

$$\langle (y(t))^p \rangle \sim \exp[-p\Gamma_{\mathrm{eff}}^{(p)} t], \tag{64}$$

where

$$\Gamma_{\mathrm{eff}}^{(p)} = \Gamma - \tfrac{1}{2} p C_A. \tag{65}$$

From this equation we can see that however small C_A is there exists a value for p for which $\Gamma_{\mathrm{eff}}^{(p)}$ is negative, for which therefore, the pth moment of $y(t)$ diverges. This in turn suggests that there are always present in the ensemble of y-histories some which become arbitrarily large. The degree to which they are important is indicated by the lowest moment of y that diverges.

It is clear for example that the second moment will diverge if

$$\langle (A(0))^2 \rangle_{\mathrm{C}} \tau_A > \Gamma. \tag{66}$$

Note that even $\langle y(t) \rangle$ may diverge if the somewhat more stringent condition

$$\langle (A(0))^2 \rangle_{\mathrm{C}} \tau_A > 2\Gamma \tag{67}$$

is satisfied. When however $\Gamma_{\mathrm{eff}}^{(p)} > 0$ we can expect straining on the corresponding moment of curvature to be suppressive. For large t the competition between straining and bending should then result in a finite asymptotic value for that moment. A detailed analysis of the solutions of the inhomogeneous equation does indeed confirm this conclusion.

The final picture is then as follows. For a period less than the velocity field correlation time the r.m.s. curvature increases linearly with time t. Subsequently, if there is a range of time for which the bending term dominates, it will increase as $t^{\frac{1}{2}}$. Finally, depending on the precise values of certain Lagrangian parameters it should either settle down to a limiting value or show an exponential divergence with time. This latter situation is the one encountered by Pope *et al.* (1989) who have examined this situation closely. The numerical results we present in §5 also support such a scenario.

We conclude this section with a caveat concerning the derivations of (37) and (46). In both cases it has been assumed that the vector quantities such as $\boldsymbol{n}$ and $\boldsymbol{e}$ are differentiable in time. This is not necessarily so. For $\boldsymbol{n}$ in the case of (37), this differentiability may break down when the curvature vanishes. For the principal curvatures of the surface element it must be acknowledged that there may exist some points where they coincide in value. Under these circumstances the principal vectors with which they are associated may change discontinuously. There does not seem to be any way of ensuring that this does not happen. One presumes in effect that such discontinuous events are sufficiently rare that they do not vitiate the statistical argument.

4. The velocity field ensemble

The turbulence was represented by an incompressible random velocity field which was chosen from a Gaussian distribution according to ideas of Kraichnan (1970), and Drummond *et al.* (1984). In order to make the calculations a little easier the autocorrelation function was chosen to be of a simple kind and was characterized by only one length- and timescale. However, the simulation does not depend for its success on this choice of spectrum for the turbulence or on the precise number of relevant timescales. All the computations were carried out at the Rutherford Laboratory, Abingdon, and at the Department of Applied Mathematics and Theoretical Physics, Cambridge. At the Rutherford Laboratory we used an AMT-DAP 510, a 32×32 array-processor. In Cambridge we used an AMT-DAP 610, a 64×64 array-processor.

The velocity field $\boldsymbol{u}(\boldsymbol{x}, t)$ is generated as a sum of Fourier components, each of which is determined by certain parameters distributed according to various probability distributions. A typical member of the velocity field ensemble in three-dimensional space is then realized by

$$\boldsymbol{u}(\boldsymbol{x},t) = a \sum_{n=1}^{N} (\boldsymbol{f}^n \cos(\psi^n) - \boldsymbol{g}^n \wedge \hat{\boldsymbol{k}}^n \sin(\psi^n)) \wedge \boldsymbol{k}^n \cos(\boldsymbol{k}^n \cdot \boldsymbol{x} + \omega^n t + \phi_n) + (\boldsymbol{g}^n \cos(\psi^n) + \boldsymbol{f}^n \wedge \hat{\boldsymbol{k}}^n \sin(\psi^n)) \wedge \boldsymbol{k}^n \sin(\boldsymbol{k} \cdot \boldsymbol{x} + \omega^n t + \phi^n), \quad (68)$$

where $\boldsymbol{k}^n$ is distributed uniformly on a sphere with radius k_0, ω^n is chosen from a Gaussian distribution $P(\omega) = (2\pi\omega_0)^{-\frac{1}{2}} \exp(-\omega^2/2\omega_0)$, ψ^n is an adjustable helicity parameter which we set to $\psi^n = \psi$ for all n and $\psi \in [0, \frac{1}{4}\pi]$, $\boldsymbol{f}^n$, $\boldsymbol{g}^n$ are distributed uniformly and independently over the unit sphere, ϕ^n is distributed uniformly and independently between 0 and 2π, a is a normalization factor $a = (3/2N)^{\frac{1}{2}} u_0/k_0$. The number N of Fourier components was usually 32, but other values of N have been studied for comparison, as well.

The method of simulation comprises choosing a set of flows and following a number of particles distributed in different configurations in the flow in such a way that two nearest neighbours are separated by at least two correlation lengths of the flow field initially. Array-processors are particularly suited for these calculations as 1024 or 4096 particles could be followed at once. At each time step the particle position and the spatial derivatives were calculated and the relevant quantities of interest were evaluated. As an integration procedure we used an algorithm based on ideas of Burlisch and Stoer (Press *et al.* 1986).

The ensemble size used to evaluate the quantities of interest normally comprised a total of 2×10^5 particles distributed over 200 velocity fields. In a given velocity field the particles were initially separated by at least two correlation lengths in order to ensure statistical independence.

5. Numerical results on the time evolution of curvature

Using the velocity field ensemble as described in the previous section we calculated the time evolution of the mean curvature of a line element. In §3 we have seen that we expect the mean curvature to increase linearly with time for small times. For our particular model we can evaluate (49) and find

$$\langle \kappa^2 \rangle \approx \tfrac{6}{35} u_0^2 k_0^4 t^2. \quad (69)$$

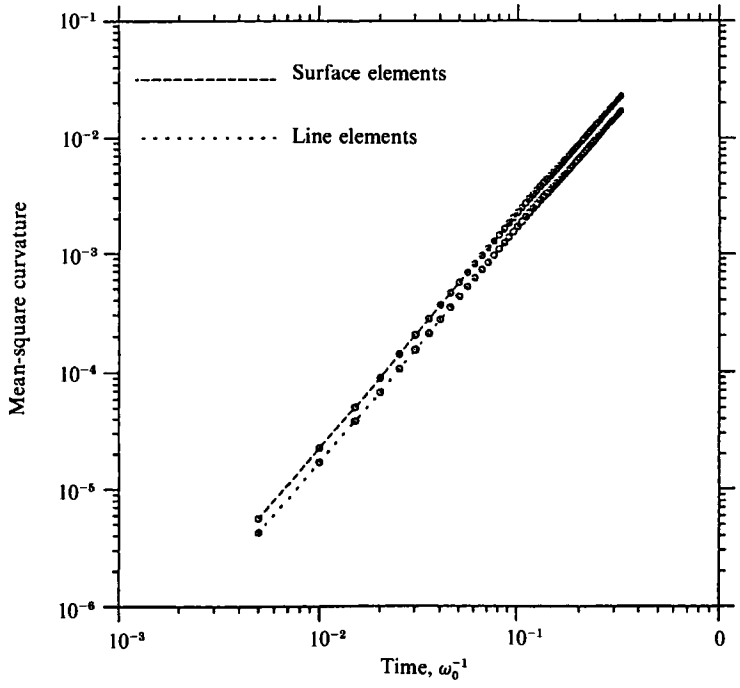

FIGURE 1. The mean-square curvature $\langle \kappa^2 \rangle$ of a line element and the sum of the two squared principal curvatures $\langle k_1^2 + k_2^2 \rangle$ of a surface element versus time for $u_0 k_0 = \omega_0 = 1$.

Furthermore in §3 we have that in the presence of isotropic turbulence the averaged equations (37) and (46) should yield similar results. We therefore predict that using (50) for short times we have

$$2\langle k^2 \rangle = \langle k_1^2 + k_2^2 \rangle \approx \tfrac{8}{35} u_0^2 k_0^4 t^2. \tag{70}$$

In figure 1 we show the numerical results for both $\langle \kappa^2 \rangle$ and $\langle k^2 \rangle$. We plot the mean-square values of the curvature normalized by $u_0^2 k_0^4$ as a function of the time t measured in terms of the correlation time of the velocity field. We see that $\langle \kappa^2 \rangle^{\frac{1}{2}}$ and $\langle k^2 \rangle^{\frac{1}{2}}$ increase linearly with time t and the coefficient is well established within the statistical errors.

For times large compared to the correlation of the velocity field the evolution of the mean curvature depends on the details of the statistics of the turbulence. In §3 we have seen that for times large compared to the correlation time of the velocity field but small compared to the curvature suppression timescale Γ^{-1} introduced in (61) the mean curvature increases proportional to $t^{\frac{1}{2}}$. As Γ^{-1} is roughly of the order of $\omega_0/(u_0 k_0)^2$ we expect this assumption to be particularly valid in the Markovian limit where the correlation time of the velocity field is much smaller than the eddy circulation time. In figure 2 we plot the numerical results for $\langle \kappa^2 \rangle$ and $\langle k^2 \rangle$ as a function of time in terms of the correlation time of the velocity field. For the case when the eddy circulation time is 10 times bigger than the correlation time of the velocity field we see that both $\langle \kappa^2 \rangle$ and $\langle k^2 \rangle$ increase linearly with time when $\omega_0^{-1} \ll t \ll \omega_0 (u_0 k_0)^{-2}$.

Figure 3 shows the time dependence of $\langle \kappa^2 \rangle^{\frac{1}{2}}$ and $\langle k^2 \rangle^{\frac{1}{2}}$ for the case $u_0 k_0 = \omega_0$. Again we see the linear dependence with time in the early part of the graph. In the later stages of the time development we do not see a levelling off with an approach to an asymptotic value. The implication of these results is that for our particular

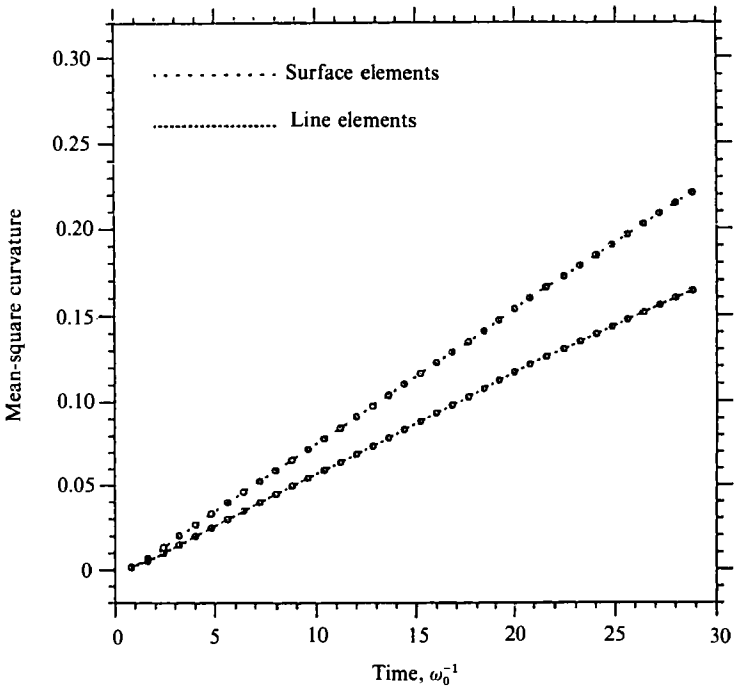

FIGURE 2. The mean-square curvature $\langle \kappa^2 \rangle$ of a line element and the sum of the two squared principal curvatures $\langle k_1^2 + k_2^2 \rangle$ of a surface element versus time for $u_0 k_0 = 0.02$, $\omega_0 = 1$.

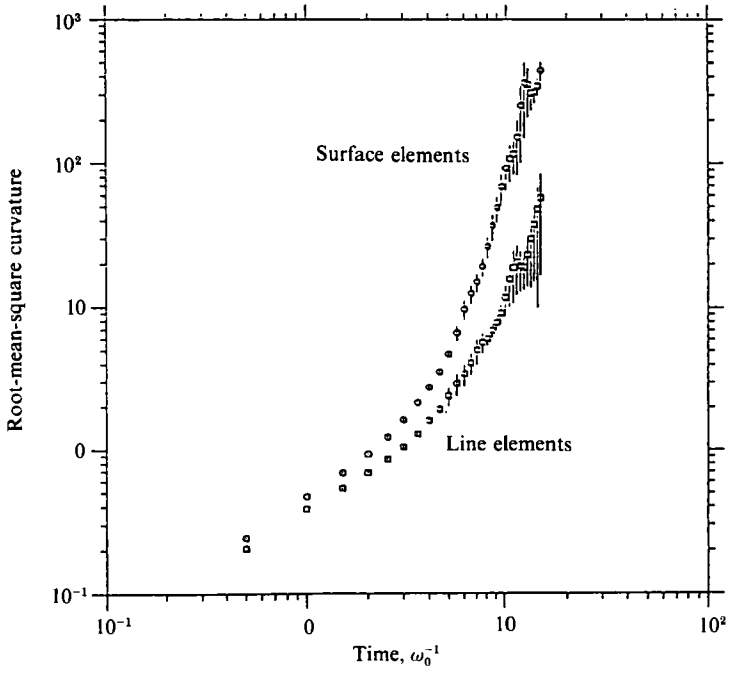

FIGURE 3. The r.m.s. curvature $\langle \kappa^2 \rangle^{\frac{1}{2}}$ for line elements and $\langle k_1^2 + k_2^2 \rangle^{\frac{1}{2}}$ for surface elements versus time for $u_0 k_0 = \omega_0 = 1$.

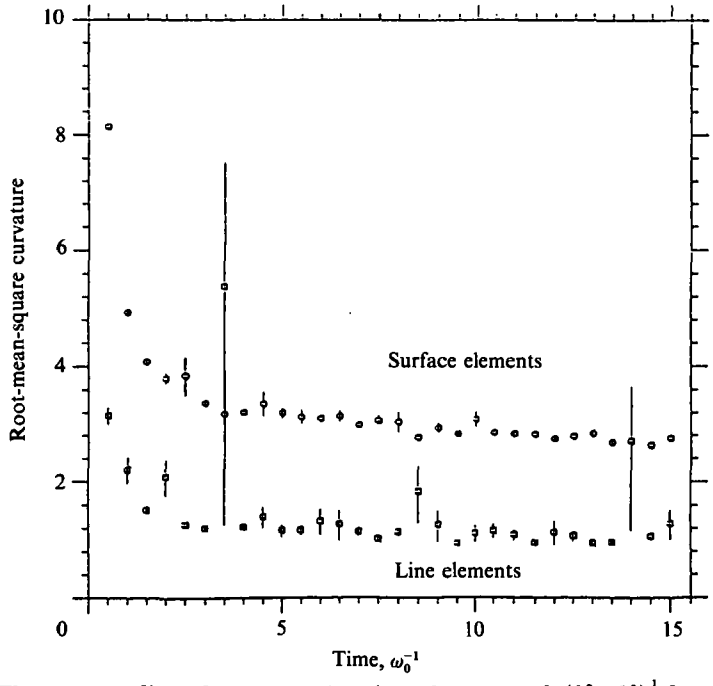

FIGURE 4. The r.m.s. radius of curvature in a line element and $\langle k_1^2 + k_2^2 \rangle^{\frac{1}{2}}$ for surface elements versus time for $u_0 k_0 = \omega_0 = 1$.

parameter values the exponent $\Gamma_{\text{eff}}^{(2)}$ for the second moment of curvature is negative, leading to an associated exponential divergence of the r.m.s. curvature with time. This is consistent with the results obtained by Pope *et al.* (1989) in their simulation of area element bending based on different models of turbulent flow. We have also measured the time development of the r.m.s. radius of curvature. This quantity suppresses the influence of very highly curved line elements. The results are shown in figure 4 and strongly suggest the emergence of an asymptotic value for the radius of curvature. This is consistent with the results obtained by Pope *et al.* (1989) on the distribution function for radius of curvature, which show a fixed distribution with a part in the neighbourhood of zero radius gradually filling with time.

6. Torsion

From the definition in (2) we see that the torsion is a pseudoscalar quantity and its sign depends on the orientation of the three vectors $\boldsymbol{t}$, $\boldsymbol{n}$ and $(\partial/\partial s)\boldsymbol{n}$, namely the tangent, normal and the direction of change of the normal along the line element. We expect therefore the mean torsion to depend on the presence of helicity in the turbulence and to vanish when the helicity is zero. This is analogous to the argument appropriate to turbulent plasmas that the α-parameter which controls the spontaneous growth of magnetic fields, also a pseudoscalar quantity, acquires a non-zero value when helicity is present in the turbulence. For our model we have in particular

$$\left.\begin{aligned} h &= \langle u_i(\boldsymbol{x},t)\,\omega_i(\boldsymbol{x},t)\rangle, \\ &= k_0 \sin 2\psi \langle u_i(\boldsymbol{x},t)\,u_i(\boldsymbol{x},t)\rangle, \\ &= u_0^2 k_0 \sin 2\psi. \end{aligned}\right\} \tag{71}$$

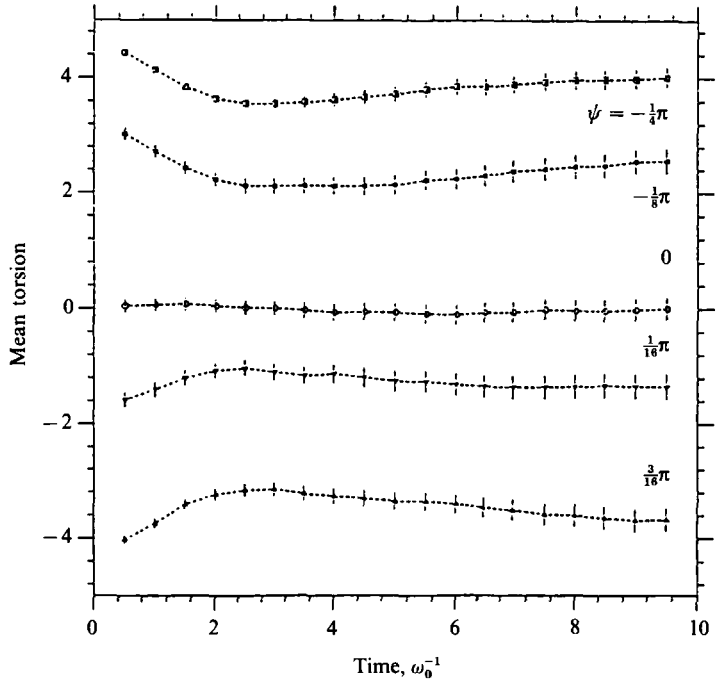

FIGURE 5. The mean torsion versus time for $u_0 k_0 = \omega_0 = 1$ and various values of the helicity parameter ψ.

Therefore we expect to find that the mean torsion vanishes for $\psi = 0$. As soon as we set $\psi \neq 0$ we induce some handedness into the flow and we expect the joint statistical distribution of the three vectors $\boldsymbol{t}$, $\boldsymbol{n}$ and $(\partial/\partial s)\boldsymbol{n}$ to reflect this fact so that given the oriented plane spanned by any two of them the third will tend to lie more on one side than the other. Thus when $\psi \neq 0$ we will find also $\langle \tau \rangle \neq 0$. For different values of ψ we show $\langle \tau \rangle$ as a function of the time t in figure 5. It is striking that $\langle \tau \rangle$ appears to reach a constant asymptotic value.

An analysis of a kind similar to that in §3 for the curvature of a line element is possible for the torsion or the squared torsion, as well. This analysis, however, does not reveal any simple relationship between, say, the curvature or the stretching and the torsion of a line element. In fact, even for short times the development of torsion depends crucially on the initial shape of the line element and the local velocity field configuration. To see this, consider (21):

$$\tau = \frac{\boldsymbol{l} \wedge \boldsymbol{a} \cdot \boldsymbol{b}}{(\boldsymbol{l} \wedge \boldsymbol{a})^2}.$$

If the line element contains a large amount of curvature the development of torsion tends to be somewhat suppressed. If we start with a line element which is rather straight we find that almost any amount of torsion can develop in very little time owing to curvature fluctuations. From a dimensional analysis of (21) it is possible to argue that the mean-square torsion $\langle \tau^2 \rangle$ does not grow exponentially in time for times larger than the correlation time of the velocity field. In figure 6 we plot the r.m.s. torsion $\langle \tau^2 \rangle^{\frac{1}{2}}$ as a function of time for different helical flows. These results show that the r.m.s. torsion grows strongly with time and that helicity has only a slight effect on this time development. We arrive then at a picture in which the turbulence

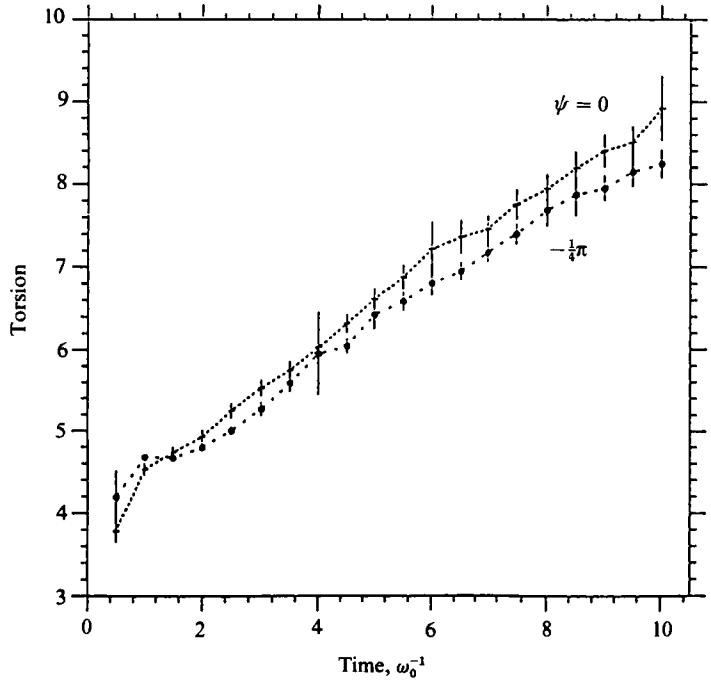

FIGURE 6. The r.m.s. torsion versus time for $u_0 k_0 = \omega_0 = 1$. The helicity parameter was chosen to be $\psi = 0$ and $\psi = \frac{1}{4}\pi$.

generates increasing amounts of torsion with or without helicity. The balance between left or right torsion, however, is controlled by the helicity.

7. Numerical results for stretching, curvature, and torsion correlations

An interesting question is the impact of stretching on curvature. Intuitively, one would expect that in regions where the line elements are stretched the creation of curvature is somewhat suppressed, whereas in regions where we do not have much stretching going on the line elements get bent owing to the random fluctuations of the stress tensors. In order to test this hypothesis we would like to know whether the two quantities $\dot{\xi}/\xi$ and $\dot{\kappa}/\kappa$ are correlated, where $\dot{\xi}/\xi$ contains the information of how fast a line element is being stretched at time t normalized by its length and $\dot{\kappa}/\kappa$ contains the information of how fast a line element changes its curvature relative to its curvature. According to the above hypothesis we expect the correlation of these two quantities to be negative. In figure 7 we plot the correlation coefficient of these two quantities as a function of time t. The correlation coefficient $r_{a,b}$ of two quantities a and b is defined as

$$r_{a,b} = \frac{\langle ab\rangle - \langle a\rangle\langle b\rangle}{(\langle a^2\rangle - \langle a\rangle^2)(\langle b^2\rangle - \langle b\rangle^2)}. \tag{72}$$

The numerical results clearly show a negative correlation coefficient and therefore support the hypothesis of stretching regions being different from regions where a lot of bending takes place.

Having established the idea of different regions of our flow as far as the generation of stretching and curvature is concerned we would like to find out whether the line

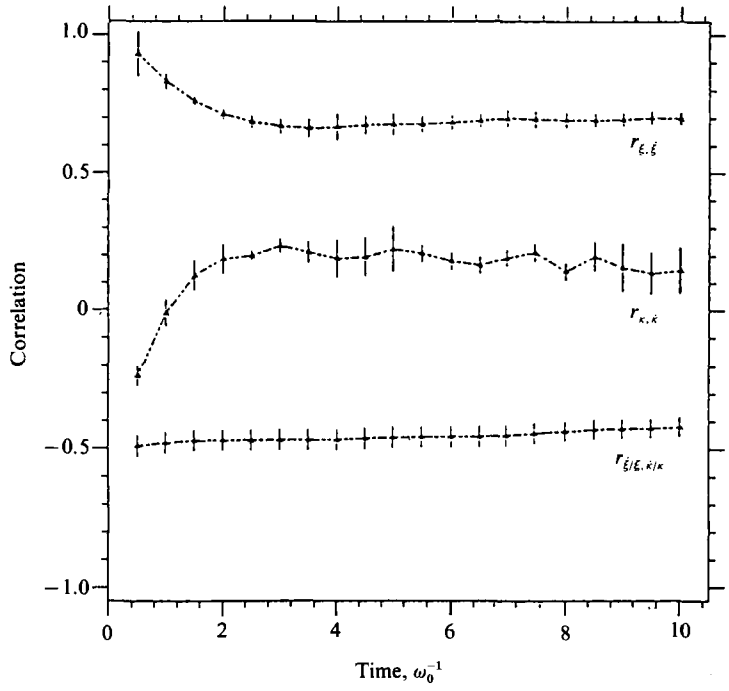

FIGURE 7. The correlation coefficients $r_{\xi,\dot{\xi}}$, $r_{\kappa,\dot{\kappa}}$, and $r_{\dot{\xi}/\xi,\dot{\kappa}/\kappa}$ versus time.

elements have a tendency to stay in either region or rather whether they wander from one to the other. To extract this sort of information we have to consider the correlation of $\dot{\xi}$ and ξ and similarly $\dot{\kappa}$ and κ. If the line elements do not have a tendency to wander from one region to the other we expect

$$r_{\dot{\xi},\xi} > 0, \tag{73}$$

i.e. long line elements are increasing their length. Similarly, curved line elements coincide with an increasing curvature and therefore

$$r_{\dot{\kappa},\kappa} > 0. \tag{74}$$

The numerical results in figure 7 seem to suggest that situations where line elements stay in any of the two regions without wandering are statistically somewhat preferred.

We measured the correlations between the torsion τ and the squared torsion τ^2 of a line element, as well. All the correlations between the torsion or the squared torsion and the stretching and curvature seem to vanish in our model. This suggests that torsion can be generated equally well at any point in the flow.

8. Conclusions

We have studied the development of curvature in line and surface elements in a manner similar to that of Pope (1988) and Pope *et al.* (1989). Our results are consistent with the conclusions of these investigations. We have shown that the equation governing the time evolution of the curvature of a line element has the same form as the equations governing the time development of the extrinsic principal curvatures of a surface patch. We therefore expect that in the case of isotropic

turbulence both the curvature of a line element and the extrinsic principal curvatures of a surface element behave similarly. Using a simple model turbulence we were able to show this equivalence numerically. Furthermore we confirmed by theoretical analysis the possibility of exponential growth of curvature induced by fluctuations of the strain tensor that was discovered by Pope *et al.* (1989). The results of our numerical simulation are consistent with this outcome.

We investigated numerically the dependence of the torsion on time in the turbulent flows and demonstrated the response of the mean torsion to the presence of helicity. The r.m.s. torsion is insensitive to helicity and appears to exhibit power law growth in time.

By measuring some of the correlation functions of the quantities involved we demonstrated that there are different regions in the flow where on the one hand the generation of curvature is suppressed and line or surface elements predominantly increase in length or surface area and, on the other hand, there are regions where curvature is generated and the growth of a line or surface element is suppressed. Furthermore we were able to show that line or surface elements have a tendency to stay in either region than wander from one to the other. The generation of torsion, however, does not correlate with any of these identified regions.

This work was supported by the EEC Twinning Contract ST2J-0029-1-F. We would like to thank Professor S. B. Pope for an extremely helpful discussion.

REFERENCES

DRUMMOND, I. T., DUANE, S. & HORGAN, R. R. 1984 Scalar diffusion in simulated helical turbulence with molecular diffusivity. *J. Fluid Mech.* **138**, 75.

DRUMMOND, I. T. & MÜNCH, W. 1990 Turbulent stretching of line and surface elements. *J. Fluid Mech.* **215**, 45.

KRAICHNAN, R. H. 1970 Diffusion by a random velocity field. *Phys. Fluids* **13**, 22.

POPE, S. B. 1988 The evolution of surfaces in turbulence. *Intl J. Engng Sci.* **26**, 445.

POPE, S. B., YEUNG, P. K. & GIRIMAJI, S. S. 1989 The curvature of material surfaces in isotropic turbulence. *Phys. Fluids* A **1**, 2010.

PRESS, W. H., FLANNERY, B. P., TEUKOLSKY, S. A. & VETTERLING, W. T. 1986 *Numerical Recipes*. Cambridge University Press.